

OPEN ACCESS

EDITED BY Fei Hao, Northumbria University, United Kingdom

REVIEWED BY
Karima Mahmoud,
National Research Centre, Egypt
Graciela Pedrana,
Universidad de la República, Uruguay

*CORRESPONDENCE
Yiming Sulaiman

☑ ysulaiman@xjau.edu.cn

[†]These authors have contributed equally to this work and share first authorship

RECEIVED 19 April 2025 ACCEPTED 01 September 2025 PUBLISHED 24 September 2025

CITATION

Muhetaer A, Gong G, Ye Y, Kuxitaer A, Zhu M, Li Q, Du X and Sulaiman Y (2025) Differential expression analysis of IncRNA and mRNA in ovarian tissues of Pishan Red Sheep and Hu Sheep with distinct genotypes during estrus.

Front. Vet. Sci. 12:1614599. doi: 10.3389/fvets.2025.1614599

COPYRIGHT

© 2025 Muhetaer, Gong, Ye, Kuxitaer, Zhu, Li, Du and Sulaiman. This is an open-access article distributed under the terms of the Creative Commons Attribution License (CC BY). The use, distribution or reproduction in other forums is permitted, provided the original author(s) and the copyright owner(s) are credited and that the original publication in this journal is cited, in accordance with accepted academic practice. No use, distribution or reproduction is permitted which does not comply with these terms.

Differential expression analysis of lncRNA and mRNA in ovarian tissues of Pishan Red Sheep and Hu Sheep with distinct genotypes during estrus

Aisima Muhetaer^{1†}, Gao Gong^{1†}, Yaoyang Ye¹, Ayipare Kuxitaer¹, Mengting Zhu¹, Qifa Li², Xing Du² and Yiming Sulaiman^{1*}

¹College of Animal Science, Xinjiang Agricultural University, Ürümqi, China, ²College of Animal Science and Technology, Nanjing Agricultural University, Nanjing, China

Pishan Red Sheep and Hu Sheep are sheep breeds with exceptional reproductive characteristics. To investigate the similarities and differences in the expression of reproduction-related genes between these two breeds, this study utilized transcriptome sequencing to identify differentially expressed lncRNAs and mRNAs in ovarian tissues during estrus in Hu Sheep and Pishan Red Sheep carrying FecB^{B+} and FecB++ genotypes. Furthermore, we explored their potential impacts on fertility. Transcriptome sequencing of ovarian tissues generated 204.58 Gb of clean data. Bioinformatics analysis identified 34,651 lncRNAs, with differential expression analysis revealing 1,481 differentially expressed mRNAs and 698 differentially expressed IncRNAs. Differentially expressed RNAs associated with reproductive performance trends were screened through expression trend analysis. Functional enrichment analysis of target genes for these mRNAs and IncRNAs revealed significant enrichment in KEGG pathways such as "Cytokine-cytokine receptor interaction," "Hippo signaling pathway" and "MAPK signaling pathway" Key candidate mRNAs were identified, including GDF9, GRIA4, HOXC9, HOXD3, MAPK8IP3, AMH, ANGPT2, FGF14, MAPK8IP1, MMP9, and BRINP3. Additionally, critical regulatory relationships between IncRNAs and mRNAs were uncovered. For example, MSTRG.61044.1 exhibited high expression in FecB++ genotype Pishan Red Sheep and may act as a hub regulator in follicular selection and hormonal responses by cis-regulating MAPK8IP1 and trans-regulating AMH, CCL25, MSTRG.23016.1 may regulate genes such as MMP9 and ANGPT2, potentially participating in the modulation of the ovarian tissue remodeling microenvironment. In contrast, MSTRG.15154.3 cis-regulates ERBB4 to modulate the granulosa cell proliferation and differentiation process. The specifically highly expressed MSTRG.2677.1 in Hu Sheep may be involved in maintaining ovarian stromal cell homeostasis through trans-regulation of HGF and BRINP3, MSTRG.27015.1 and MSTRG.60286.1 target MAPK8IP3 and PPP3CB respectively, suggesting their potential roles in cell cycle regulation and oocyte maturation. These findings provide important molecular mechanisms and potential regulatory targets for improving reproductive performance in sheep.

KEYWORDS

Pishan Red Sheep, Hu Sheep, ovary, transcriptome, reproductive performance

1 Introduction

Pishan Red Sheep and Hu Sheep, as two important indigenous sheep breeds in China, have attracted significant attention due to their distinctive reproductive characteristics. Pishan Red Sheep are particularly renowned for their prolificacy, with notable differences in the expression of reproduction-associated genes observed between different lambing types (1). ChengLong et al. (1) demonstrated that in extreme environments, the population structure and genetic diversity of Pishan Red Sheep significantly influence their reproductive performance, with their prolific lambing traits being particularly prominent. Hu Sheep, characterized by their "year-round estrus and high prolificacy," serve as an ideal model for studying the mechanisms underlying high fecundity (2). Relevant studies indicate that Hu Sheep, as a prolific sheep breed, can achieve a lambing rate exceeding 200% under optimal feeding conditions (3).

The litter size trait in mammals is governed by an integrated reproductive system, representing a complex quantitative trait regulated by multiple factors including genetics, environmental conditions, and hormonal levels (4). In sheep, litter size exhibits relatively low heritability, yet selective breeding through conventional methods can progressively enhance this trait and improve overall flock reproductive performance (5). With advancements in biotechnology, marker-assisted selection (MAS) has provided new opportunities to enhance selection efficiency for improving litter size in sheep (6). Long non-coding RNAs (lncRNAs) play critical regulatory roles in ovarian function and estrous cycle regulation in sheep (7). lncRNAs regulate gene expression through multiple mechanisms, including miRNA interactions (8), modulation of mRNA stability and translation efficiency (9), and epigenetic modification-mediated gene regulation (10). During the estrous cycle in sheep, the lncRNA expression profiles in ovarian tissues undergo dynamic changes, which may be functionally associated with follicular maturation, ovulation, and corpus luteum formation (11).

Litter size in sheep is regulated by the integrated ovarian reproductive system through diverse physiological and molecular mechanisms, including sex hormone secretion, follicular development and maturation, as well as lncRNA-mediated expression control of key genes (6). In sheep reproduction, the ovaries serve as one of the pivotal organs governing litter size (12). Through the secretion of sex hormones (e.g., estrogen and progesterone) and oocyte production, the ovaries regulate the reproductive cycle (13). During the estrous cycle, ovarian follicles undergo developmental progression from primordial to mature stages, culminating in oocyte release during ovulation (14). This process is precisely regulated by the hypothalamic-pituitary-ovarian (HPO) axis, with gonadotropin-releasing hormone (GnRH), follicle-stimulating hormone (FSH), and luteinizing hormone (LH) playing pivotal roles (15).

Advances in high-throughput sequencing technologies have accelerated research on the functional roles of lncRNAs in ovarian regulation of sheep reproduction (11, 16). Sheep with different FecB genotypes exhibit significant variations in reproductive performance (1), where $FecB^{B+}$ carriers demonstrate superior litter size traits compared to $FecB^{++}$ genotypes. Studies demonstrate that $FecB^{B+}$ sheep exhibit significantly higher litter sizes (1.453 \pm 0.063) compared to $FecB^{++}$ genotypes (1.125 \pm 0.059) (17). Existing studies have identified extensive differentially expressed genes (DEGs) across multiple tissues and blood transcriptomes among sheep with distinct FecB genotypes

(18). Hu Sheep exhibit stable reproductive performance (19). As a representative prolific breed, their transcriptomic data provide critical references for comparative analyses (20). Current research on differential expression of lncRNAs and mRNAs in ovarian tissues during estrus between Pishan Red Sheep and Hu Sheep remains limited, particularly in comparative studies of different *FecB* genotypes. The regulatory networks and their underlying biological functions have yet to be systematically elucidated.

This study aims to delineate the regulatory mechanisms underlying ovarian physiology through comparative transcriptomic profiling of differentially expressed long non-coding RNAs (lncRNAs) and mRNAs in ovarian tissues during the estrous cycle between Pishan Red Sheep and Hu Sheep. Through systematic integration of lncRNA-mRNA co-expression networks, this investigation elucidates their functional interplay in modulating ovarian homeostasis, thereby establishing a molecular framework for enhancing ovine reproductive efficiency and informing marker-assisted selection strategies in genetic improvement programs.

2 Materials and methods

2.1 Animals and sample collection

The experimental animals used in this study, Hu Sheep and Pishan Red Sheep, were provided by Xiyu Muyangren Agriculture and Animal Husbandry Co, Ltd. in Pishan County, Hotan Prefecture. Experimental ewes were selected based on lambing records under uniform feeding conditions. The cohort comprised Hu Sheep ($FecB^{BB}$), heterozygous $FecB^{B+}$ Pishan Red Sheep, and wild-type $FecB^{++}$ Pishan Red Sheep, all being healthy, non-related nulliparous ewes aged 7–8 months with consistent body conformation, the number of animals per group was n=4.

2.2 Estrus synchronization and experimental grouping

Estrus synchronization was performed on all 18 selected ewes using a single prostaglandin F2 α (PGF2 α)-based protocol. The luteal phase was initially confirmed through visual assessment of estrus signs. Each ewe received an intramuscular injection of 0.1 mg PGF2 α . At 48 h post-injection, estrus behavior was detected using the ram exposure method to determine optimal timing for sample collection.

2.3 Ovarian tissue collection and experimental grouping

Four estrous Pishan Red Sheep with $FecB^{B+}$ genotype (Group A), four with $FecB^{++}$ genotype (Group B), and four Hu Sheep (Group C) were selected and humanely slaughtered. Ovarian tissue samples were promptly collected, and tissues surrounding the ovaries were removed. The samples were rinsed with phosphate-buffered saline (PBS), transferred to RNase-free cryotubes, and immediately snap-frozen in liquid nitrogen. All animal experimental procedures strictly adhered to the Institutional Animal Care and Use Guidelines of Xinjiang Agricultural University.

2.4 Experimental materials

The experiment employed the following instrumentation to meet operational requirements across all experimental stages: PCR system (Life Technologies), dry bath incubator (TIANGEN), mini centrifuge (TIANGEN), vortex mixer (Vortex-Genie 2, Scientific Industries), adjustable pipettes (RAININ), magnetic separation rack (Life Technologies), tube rotator (QLinbeier), Qsep-400 automated electrophoresis system (BiOptic Inc.), and Qubit 3.0 Fluorometer (Thermo Fisher Scientific).

2.5 RNA extraction and library construction

Total RNA was extracted from ovine ovarian tissues using TRIzol reagent (Thermo Fisher Scientific, USA). RNA concentration was measured with a NanoDrop 2000 spectrophotometer (Thermo Fisher Scientific, USA), while RNA integrity was assessed using an Agilent 2,100 Bioanalyzer (Agilent Technologies, USA). Library quality control was performed with the Qsep-400 system (BiOptic Inc., Taiwan, China). Qualified libraries were subsequently sequenced on the NovaSeq X Plus platform (Illumina, USA) with 150 bp paired-end reads. The RNA-Seq data of Pishan Red Sheep and Hu Sheep have been deposited in the Sequence Read Archive (SRA) database of the National Center for Biotechnology Information (NCBI) under BioProject accession number PRJNA1226111.

2.6 Screening of differentially expressed mRNAs and IncRNAs in ovarian tissues

Following sequencing, the data were analyzed using the bioinformatics pipeline provided by the BMKCloud platform¹ from Biomarker Technologies. The FASTQ data obtained from highthroughput sequencing were analyzed to predict and identify multiple RNA species, followed by quantitative profiling of distinct RNA categories through alignment with established RNA annotation databases. In this study, differentially expressed genes (DEGs) and lncRNAs were screened using stringent thresholds of Fold Change ≥ 1.5 and p-value < 0.01. Differential comparison groups: A-L vs. B-L, A-L vs. C-L, B-L vs. C-L. Target genes of lncRNAs were predicted using two distinct approaches. The first method focused on cis-regulatory mechanisms, identifying adjacent protein-coding genes located within a 100 kb genomic window upstream/downstream of lncRNA loci as potential targets, based on the positional relationship between lncRNAs and their neighboring genes. The second approach employed trans-regulatory prediction by analyzing inter-sample expression correlation between lncRNAs and mRNAs, identifying potential target genes through co-expression patterns.

2.7 Trend analysis

The differentially expressed lncRNAs and mRNAs identified were further analyzed to investigate their expression dynamics across

1 www.biocloud.net

different genotypes. Gene expression dynamics were visualized through trend analysis plots to delineate specific expression pattern alterations.

2.8 Enrichment analysis

The Gene Ontology (GO) database, established in 2000 by the Gene Ontology Consortium, constitutes a cross-species standardized annotation framework for genes and their products, structured into three orthogonal categories: Biological Process (BP), Molecular Function (MF), and Cellular Component (CC). Following gene annotation, functional categorization of differentially expressed genes (DEGs) was conducted at the second-level Gene Ontology (GO) classification. Enrichment analysis of DEG sets from each comparison group was performed using the hypergeometric test implemented in the clusterProfiler R package (v4.0.5), with results visualized as bar plots. A lower q-value indicates greater statistical significance of the enriched functional pathways, thereby facilitating the functional inference of candidate genes. Pathway enrichment analysis of differentially expressed genes was conducted using the KEGG (Kyoto Encyclopedia of Genes and Genomes) database. KEGG pathways were utilized as ontological units, and the hypergeometric test was applied to identify significantly enriched pathways (adjusted *p*-value < 0.01) by comparing against the genomic background. Concurrently, KEGG pathway annotation results for both target genes of differentially expressed lncRNAs and mRNAs were systematically categorized according to KEGG pathway classifications, thereby identifying key biochemical metabolic and signal transduction pathways in which these genes are functionally implicated. The present investigation primarily centers on biological pathways associated with reproductive physiology and ovarian functional regulation.

2.9 Screening of key mRNAs and IncRNAs

This study implemented an integrated methodology combining systematic literature review and multi-omics database mining to identify functionally pivotal genes associated with ovine reproductive performance. The selection criteria prioritized core constituents within key reproductive pathways, including the estrogen signaling pathway, MAP kinase cascade, cytokine-cytokine receptor interaction, and Hippo signaling pathway. Corresponding nucleotide sequences and spatiotemporal expression profiles were retrieved from the NCBI GenBank and GEO database. Differential expression analysis of mRNA and lncRNA was conducted using DESeq2 and edgeR packages on ovarian tissue samples from *FecB*⁺⁺-genotype Pishan Red Sheep, *FecB*^{B+}-genotype Pishan Red Sheep, and Hu Sheep, based on high-throughput sequencing data to identify genes with statistically significant expression changes.

2.10 Integrated analysis of hub mRNAs and key lncRNAs

During the integrated analysis of hub mRNAs and key lncRNAs, significantly differentially expressed mRNAs and lncRNAs were first identified. Subsequently, a cross-correlation heatmap was constructed to visualize expression covariation patterns between these two RNA classes.

2.11 Real-time quantitative fluorescence

To validate the expression levels of key candidate genes identified from screening, we performed qRT-PCR analysis on additional ovine ovarian tissue samples, thereby confirming the reliability of both sequencing and bioinformatics results. Using β -Actin as the internal reference, the relative gene expression levels were calculated for each sample and group. The processed data were organized in Excel and subsequently analyzed for visualization using Origin 2024 software. Primer sequences are provided in Table 1. Primers were designed using Premier 6 (Premier Biosoft, USA) and synthesized by Biomarker Technologies (Beijing, China). cDNA was reverse transcribed from total RNA, followed by RT-PCR amplification. Quantitative PCR was performed under the following conditions: initial denaturation at 95 °C for 3 min; 39 cycles of 95 °C for 10 s (denaturation), 60 °C for 30 s (annealing/extension) with plate reading; followed by a melting curve analysis (60–95 °C, increment of 1 °C per cycle, 4 s hold time).

3 Results

3.1 Total RNA quality assessment

The detection conclusions were based on Biomarker Beijing's sequencing sample detection standard requirements and constituted a comprehensive evaluation of the tested samples. The samples with Test Result A meet the quality requirements for library construction, and the total quantity is sufficient for two or more standard library preparations. RNA quantification via NanoDrop demonstrated a concentration range of 98.9–652.8 ng/ μ L with total yields ranging from 1.48 to 9.79 μ g. RNA Integrity Numbers (RIN) were distributed between 6.1 and 8.8, while 28S/18S rRNA ratios spanned 1.0 to 4.03. Detailed mRNA extraction parameters are presented in Table 2.

3.2 Quality and alignment information of the test data

Strand-specific RNA sequencing libraries were constructed and sequenced on the NovaSeq X Plus platform (Illumina). Following

TABLE 1 List of PCR primer sequences.

Gene Name	Sequence (5' \rightarrow 3')	Product (bp)	
Q A ativ	F:CGTGCGTGACATCAAAGAGAA	141	
β-Actin	R:AACCGCTCGTTGCCAATAGT		
MMP9	F:GCACGCACGACATCTTTCAG	115	
	R:AGGAGGTCGAAGGTCACGTA		
AMH	F:GCTCATCCCCGAGACATACC	181	
	R:GATGAGGAGCTTGCCTGTGT	101	
MAPK8IP3	F:CAACACCGACTCCCTGTACC		
	R:ACGCACTGAGAACTCCCCTA	100	
ANGPT2	F:AGCACGAAGGATGCAGACAA	101	
	R:CCATTCAGGTTGGAGGGACC	101	
MSTRG.60286.1(lncRNA)	F:GGCACAGCATTTTAGTGCCT		
W51 KG.00280.1(IIICKINA)	R:CACCCAGTGGACCTTCTTCC	165	

stringent quality control, a total of 204.58 Gb clean data were obtained with Q20 > 97.45% and Q30 > 93.31%, while maintaining low N ratios and stable GC content, indicating high-quality sequencing outputs (detailed metrics in Table 3). Reference genome alignment statistics revealed mapping rates ranging from 81.40 to 91.19% against the *Ovis aries* reference genome assembly (Ovis_aries.GCF_000298735.2_Oar_v4.0.genome.fa). Complete alignment results are tabulated in Table 4.

3.3 Comparative analysis of lncRNA and mRNA in sheep ovaries with different fecundity

The coding potential of putative lncRNAs was systematically assessed using four distinct computational tools: CNCI, CPC2, Pfam Scan, and CPAT. The intersection analysis of these predictions (Figure 1A) identified 34,651 high-confidence lncRNAs with conserved non-coding features. As depicted in Figure 1B, the composition of lncRNA classes was: intergenic lncRNAs (15,611, 45.1%), antisense lncRNAs (3,462, 10%), intronic lncRNAs (15,062, 43.5%), and sense lncRNAs (516, 1.5%). As illustrated in Figure 1C, the middle ring depicts the chromosomal distribution of differentially expressed mRNAs, while the inner ring represents the chromosomal distribution of differentially expressed lncRNAs. Within the rings, red and green denote upregulated and downregulated mRNAs, respectively; yellow and blue indicate upregulated and downregulated lncRNAs, correspondingly. As shown in Figure 1D, the expression levels of lncRNAs were consistently lower than mRNAs overall. Figure 1E illustrates the transcript length distribution, revealing that lncRNAs are primarily distributed between 200 and 400 bp, whereas mRNAs predominantly range from \geq 3,000 bp.

3.4 Differential expression analysis of lncRNA and mRNA between different groups

Comparative analysis revealed distinct differential expression profiles across the three comparison groups: A-L vs. B-L (Figure 2A), A-L vs. C-L (Figure 2B), and B-L vs. C-L (Figure 2C). Specifically, 92 differentially expressed lncRNAs (56 upregulated, 36 downregulated), 269 lncRNAs (144 upregulated, 125 downregulated), and 466 lncRNAs (217 upregulated, 249 downregulated) were identified in the respective groups. Concurrently, 141 differentially expressed mRNAs (60 upregulated, 81 downregulated), 1,397 mRNAs (685 upregulated, 712 downregulated), and 1,821 mRNAs (830 upregulated, 991 downregulated) were detected in these comparisons. To comprehensively characterize the transcriptional changes in ovarian tissues during estrus, we identified differentially expressed long non-coding RNAs (lncRNAs) and messenger RNAs (mRNAs). The top five upregulated and downregulated lncRNAs and mRNAs are presented in Supplementary Tables 1 and 2, respectively. Venn analysis demonstrated that 1,481 shared differentially expressed mRNAs (Figure 2D) and 698 shared differentially expressed lncRNAs (Figure 2E) overlapped across all three groups.

TABLE 2 Information on sample mRNA extraction.

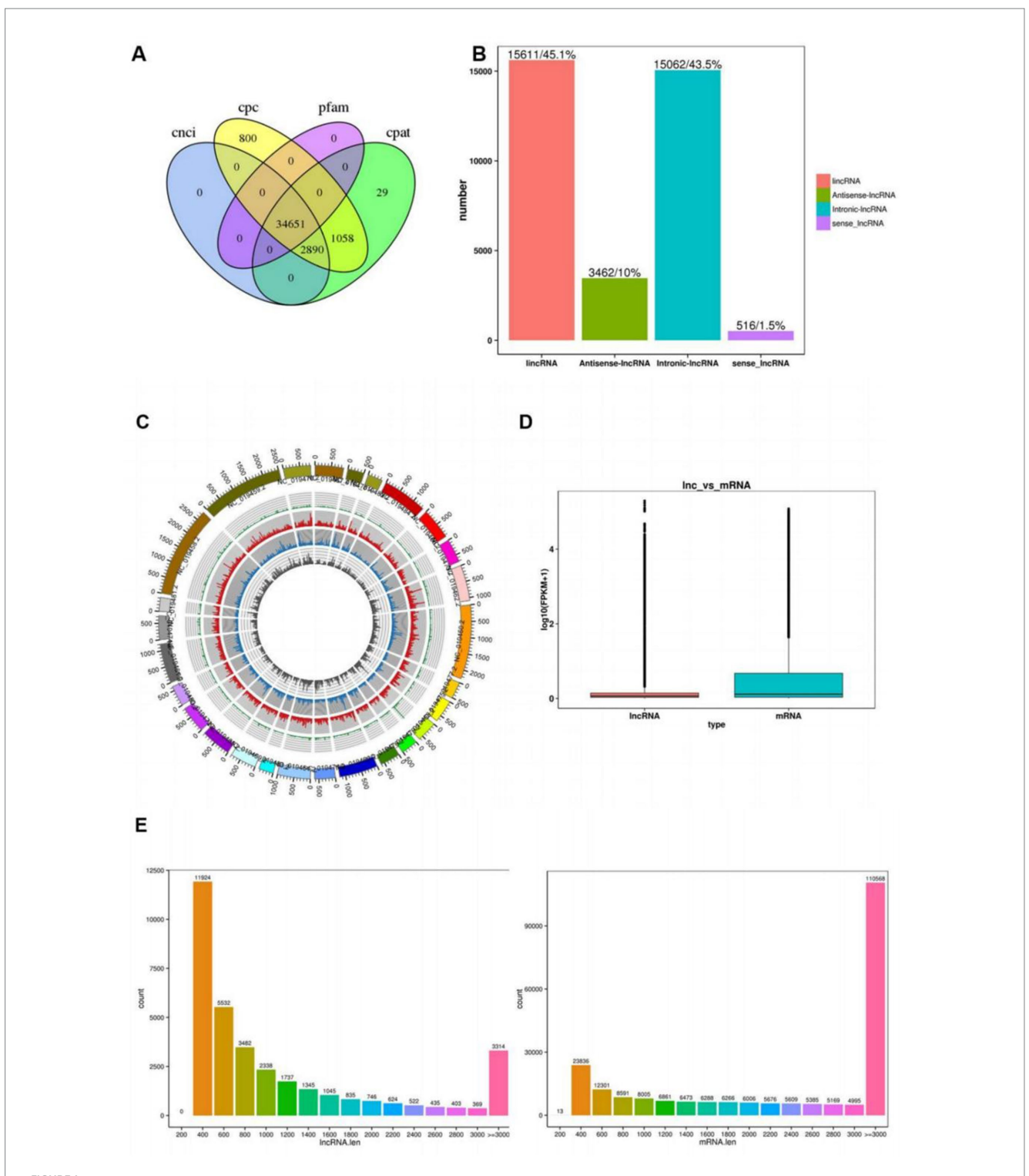
Breeds	Detection results	Nanodrop detection concentration (ng/ ul)	Volume (ul)	Total quantity (ug)	RIN value	285/185
A1-L	A	253	15	3.80	7.7	3.13
A4-L	A	517.2	15	7.76	6.8	1
A2-L	A	652.8	15	9.79	8.8	4.03
A3-L	A	302.3	15	4.53	7	3.18
B1-L	A	481.4	15	7.22	6.2	1.37
B2-L	A	189.1	15	2.84	7.2	3.03
B3-L	A	374.1	15	5.61	6.5	1.75
B4-L	A	493.9	15	7.41	6.6	1.89
C1-L	A	119.9	15	1.80	6.1	1.59
C2-L	A	455.9	15	6.84	6.7	1.74
C3-L	A	294.9	15	4.42	6.6	2.81
C4-L	A	98.9	15	1.48	6.8	1.96

TABLE 3 Assessment statistics of sample sequencing data.

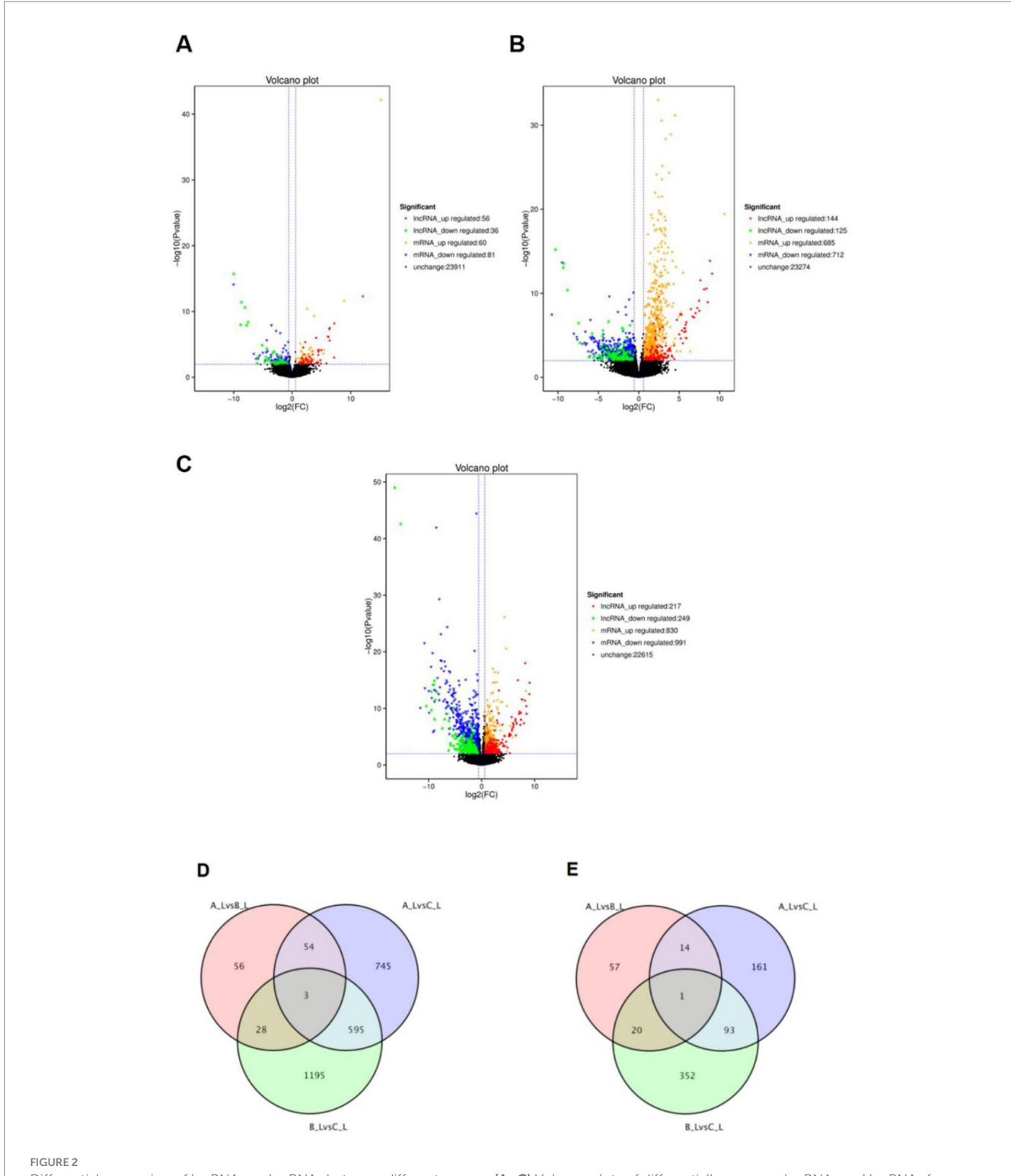
Breeds	Sample ID	Read sum	Base sum	GC (%)	N (%)	Q20 (%)	Q30 (%)
FecB ^{B+} Type Pishan Red Sheep	A1-L	55,147,707	16,507,803,237	47.07	0.02	97.76	94.06
	A2-L	56,231,640	16,824,877,240	48.12	0.02	97.84	94.25
	A3-L	55,010,326	16,452,282,004	48.72	0.02	97.65	93.98
	A4-L	57,751,857	17,264,327,636	46.37	0.01	98.06	94.74
FecB** Type Pishan Red Sheep	B1-L	55,715,053	16,671,403,429	48.69	0.02	97.48	93.64
	B2-L	55,891,691	16,702,518,965	49.71	0.02	97.60	93.82
	B3-L	57,305,418	17,145,581,750	47.05	0.02	97.87	94.35
	B4-L	57,646,787	17,257,333,335	47.01	0.02	97.80	94.08
Hu Sheep	C1-L	56,729,728	16,965,171,835	48.82	0.01	97.45	93.31
	C2-L	54,511,792	16,308,097,034	47.54	0.02	97.64	93.75
	C3-L	55,652,920	16,644,744,049	47.60	0.02	97.57	93.74
	C4-L	66,300,012	19,833,530,886	47.51	0.01	97.64	93.77

 ${\sf TABLE~4~Statistics~of~sequence~alignment~results~of~sample~sequencing~data~with~the~selected~reference~genome.}$

Breeds	Sample ID	Total reads	Mapped reads	Uniq mapped reads	Multiple mapped reads
FecB ^{B+} Type Pishan Red Sheep	A1-L	110,295,414	100,249,721 (90.89%)	93,173,782 (84.48%)	7,075,939 (6.42%)
	A2-L	112,463,280	102,181,710 (90.86%)	92,945,700 (82.65%)	9,236,010 (8.21%)
	A3-L	110,020,652	93,974,246 (85.42%)	86,584,323 (78.70%)	7,389,923 (6.72%)
	A4-L	115,503,714	105,223,523 (91.10%)	98,986,052 (85.70%)	6,237,471 (5.40%)
FecB** Type Pishan Red Sheep	B1-L	111,430,106	99,336,048 (89.15%)	90,783,819 (81.47%)	8,552,229 (7.67%)
	B2-L	111,783,382	100,305,632 (89.73%)	90,254,939 (80.74%)	10,050,693 (8.99%)
	B3-L	114,610,836	104,509,269 (91.19%)	96,483,939 (84.18%)	8,025,330 (7.00%)
	B4-L	115,293,574	103,840,153 (90.07%)	98,081,800 (85.07%)	5,758,353 (4.99%)
Hu Sheep	C1-L	113,459,456	92,351,227 (81.40%)	86,999,334 (76.68%)	5,351,893 (4.72%)
	C2-L	109,023,584	99,324,537 (91.10%)	91,705,783 (84.12%)	7,618,754 (6.99%)
	C3-L	111,305,840	99,659,995 (89.54%)	91,075,550 (81.82%)	8,584,445 (7.71%)
	C4-L	132,600,024	119,959,119 (90.47%)	110,689,067 (83.48%)	9,270,052 (6.99%)



Identification of IncRNAs and mRNAs in ovaries of sheep with different fecundity. (A) Demonstrates the coding potential of IncRNAs predicted by four bioinformatics tools: CNCI, CPC, Pfam, and CPAT; (B) The X-axis represents four distinct types of IncRNAs, The Y-axis represents the number of corresponding IncRNAs; (C) The middle ring depicts the chromosomal distribution of differentially expressed mRNAs, while the inner ring represents the chromosomal distribution of differentially expressed IncRNAs. Within the rings, red and green denote upregulated and downregulated mRNAs, respectively; Yellow and blue indicate upregulated and downregulated IncRNAs, correspondingly; (D) Displays the expression levels of mRNAs and IncRNAs, The Y-axis represents log2-transformed FPKM (Fragments Per Kilobase per Million mapped reads) values; (E) Illustrates the transcript length distribution, The Y-axis indicates the number of corresponding IncRNAs.

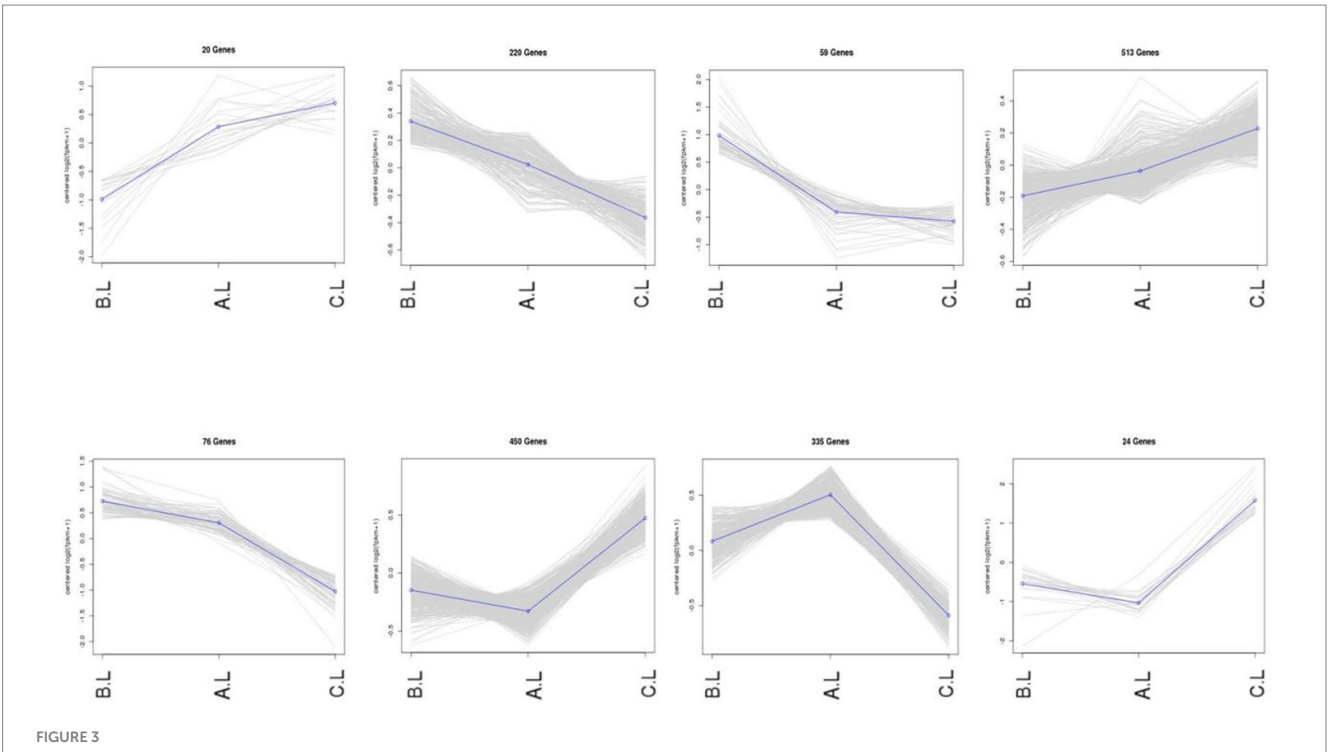


Differential expression of IncRNAs and mRNAs between different groups. (A–C) Volcano plots of differentially expressed mRNAs and IncRNAs for A-LvsB-L, A-LvsC-L and B-LvsC-L comparisons, respectively; (D) Venn diagram of differentially expressed mRNAs among A-LvsB-L, A-LvsC-L and B-LvsC-L groups; (E) Venn diagram of differentially expressed IncRNAs among A-LvsB-L, A-LvsC-L and B-LvsC-L groups.

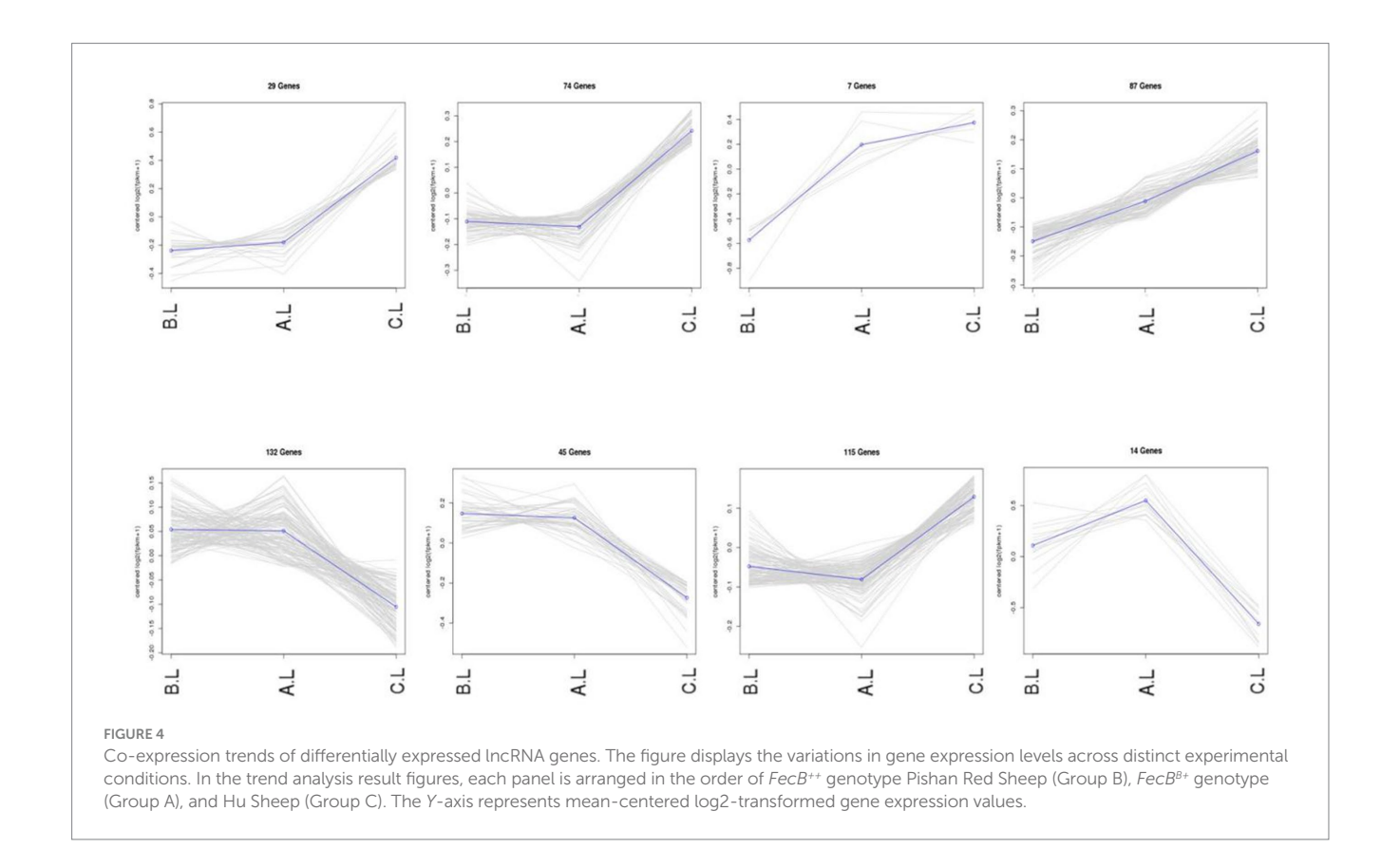
3.5 Expression trends of mRNA and lncRNA

Expression trend analysis was performed on differentially expressed mRNAs and lncRNAs (Figures 3, 4). In the trend analysis result figures,

each panel is arranged in the order of $FecB^{++}$ -genotype Pishan Red Sheep (Group B), $FecB^{B+}$ -genotype (Group A), and Hu Sheep (Group C). Clusters were selected based on the lambing performance patterns of these three types of sheep. The selection criteria were defined as



Co-expression trends of differentially expressed mRNA genes. The figure displays the variations in gene expression levels across distinct experimental conditions. In the trend analysis result figures, each panel is arranged in the order of $FecB^{++}$ genotype Pishan Red Sheep (Group B), $FecB^{B+}$ genotype (Group A), and Hu Sheep (Group C). The Y-axis represents mean-centered log2-transformed gene expression values.



follows: clusters exhibiting either consistently increasing or decreasing expression trends across all three groups, lower expression levels in Group B, but higher levels in Groups A and C, or higher expression

levels in Group B, but lower levels in Groups A and C. This screening identified 888 differentially expressed mRNAs and 6,740 differentially expressed lncRNAs conforming to these expression trends.

3.6 Prediction of IncRNA target genes

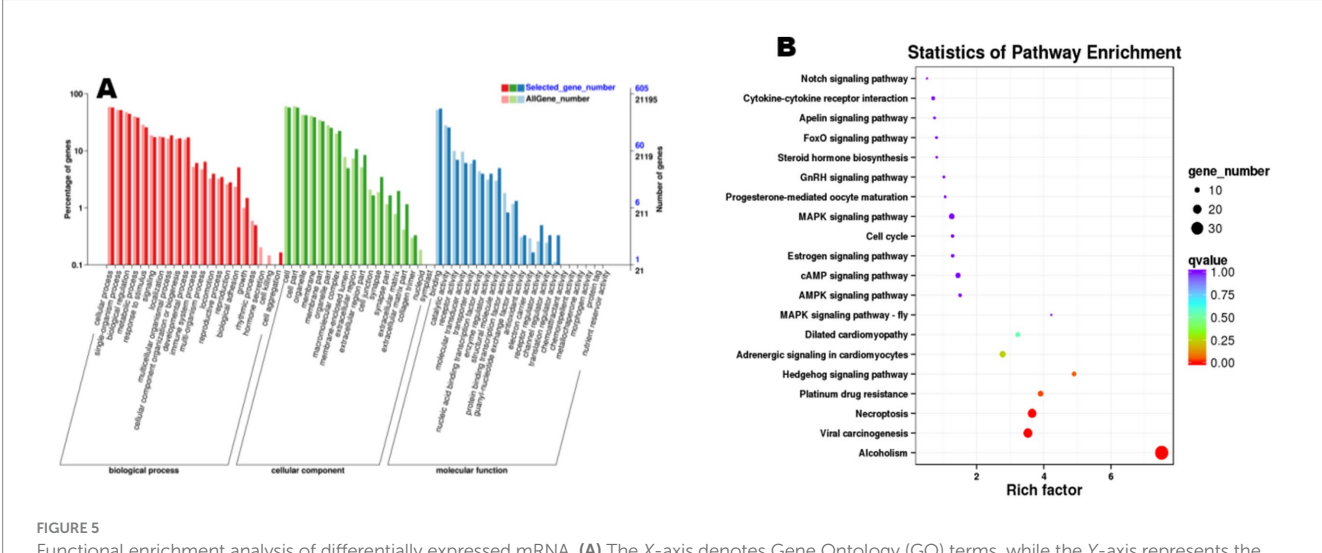
LncRNAs orchestrate a broad spectrum of critical physiological processes through transcriptional and post-transcriptional regulation of target genes. Leveraging trend-based expression profiles, we performed systematic prediction of both cis-acting and trans-regulatory target genes for these prioritized lncRNAs. Cis-regulatory target genes were predicted by identifying protein-coding genes located within ±100 kb genomic regions flanking the lncRNAs using a Perl script, yielding 845 cis-target pairs. Furthermore, trans-regulatory targets were determined through Pearson correlation analysis of inter-sample co-expression patterns between lncRNAs and mRNAs, identifying 5,895 transtarget interactions.

3.7 Functional enrichment analysis of mRNA

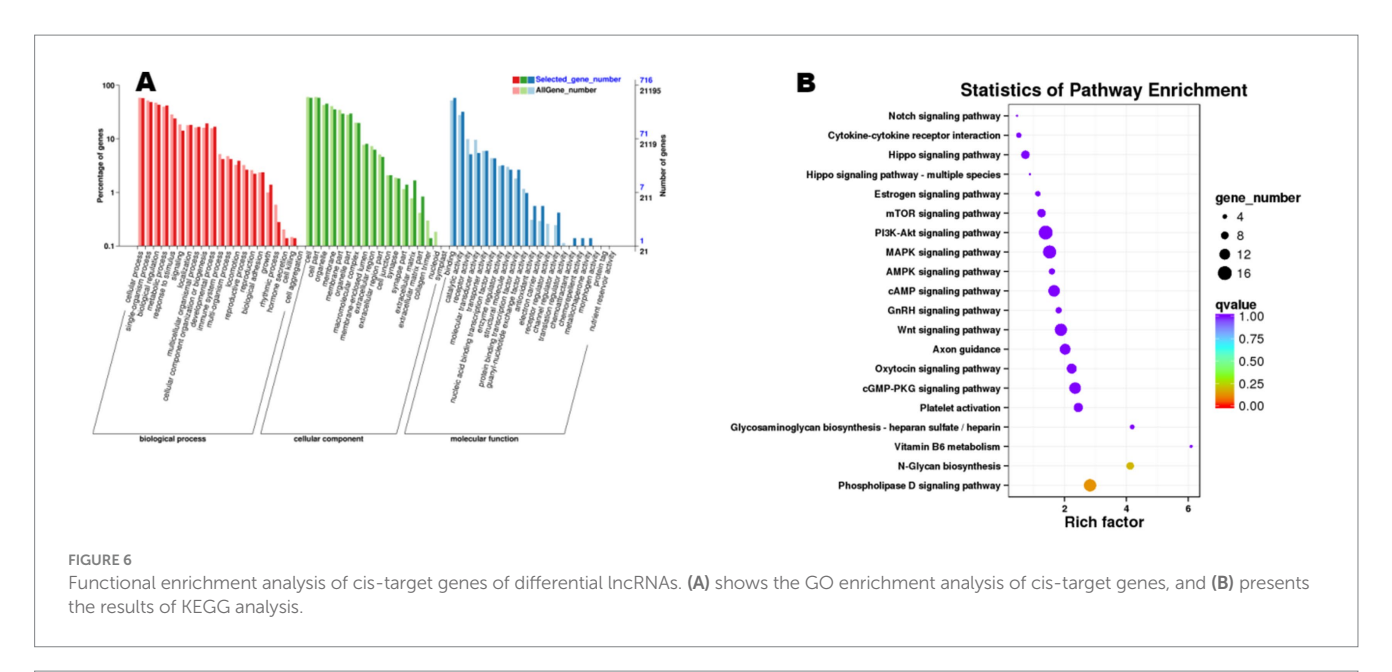
Functional enrichment analysis was performed on the 888 trending differentially expressed genes (DEGs), revealing significant enrichment of 60 GO terms and 285 KEGG pathways (Figure 5). Significant enrichments were observed in biological processes (Biological Process, BP), including key terms such as "cellular process" and "metabolic process." Furthermore, KEGG pathway analysis revealed differential enrichment across multiple pathways, including cysteine and methionine metabolism, axon guidance, and Fc gamma receptor (FcγR)-mediated phagocytosis, among others. Notably, reproduction-associated pathways including progesterone-mediated oocyte maturation, estrogen signaling pathway, and gonadotropinreleasing hormone (GnRH) signaling pathway were prominently enriched in the ovarian mRNA enrichment analysis. These findings suggest that genes within these pathways may play pivotal roles in ovarian physiological activities and reproductive regulation during the estrus phase in sheep.

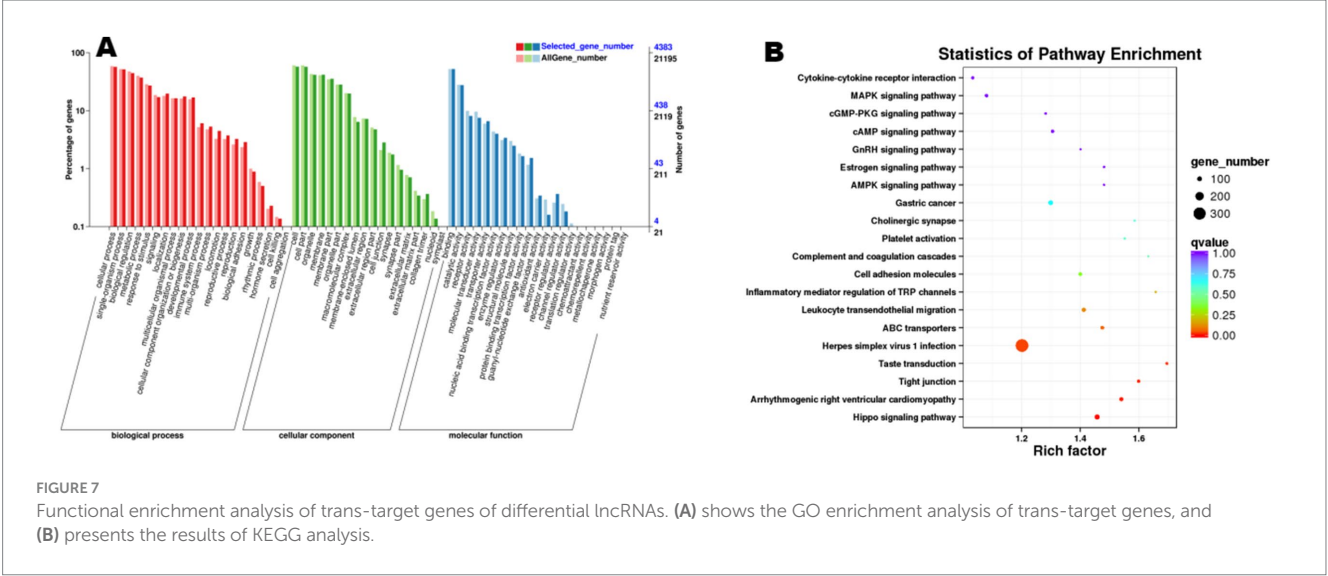
3.8 Functional enrichment analysis of ncRNA target genes

Functional enrichment analysis of the 845 cis-target genes and 5,859 trans-target genes predicted from the 6,704 trend-conforming lncRNAs revealed significant enrichments of 60 and 63 GO terms, and 289 and 330 KEGG pathways, respectively. GO enrichment analysis of cis-target genes (Figure 6) demonstrated significant enrichment in biological processes (BP), including "cellular process," "singleorganism process," "biological regulation," and "metabolic process," indicating potential functional roles of these genes in diverse biological processes within ovarian tissues. KEGG pathway analysis of cis-target genes (Figure 6) revealed differential enrichment across multiple pathways, including "Cytokine-cytokine receptor interaction," "Hippo signaling pathway," and "Estrogen signaling pathway," among others. GO enrichment analysis of trans-acting target genes (Figure 7) revealed that in the biological process category, entries such as "cellular process" and "single-organism process" exhibited relatively higher numbers of enriched lncRNA trans-acting target genes. This observation suggests that during physiological activities in ovarian tissues at the estrus phase, these biological processes may be significantly influenced by genes under trans-regulatory control of corresponding lncRNAs. KEGG pathway analysis (Figure 7) revealed significant enrichment of lncRNA trans-target genes in ovarian tissues for key pathways including "Cytokine-cytokine receptor interaction," "MAPK signaling pathway," and "cGMP-PKG signaling pathway." These findings suggest these pathways may exert central regulatory functions in ovarian physiological processes during the estrous cycle. Furthermore, pathways including the "MAPK signaling pathway" and "cAMP signaling pathway" demonstrated consistent enrichment in both cis- and trans-target gene KEGG analyses, suggesting their potential roles in regulating signal transduction, cellular proliferation, and differentiation within ovarian tissues. The co-enrichment of these pathways further elucidates the multifaceted mechanisms by which lncRNAs orchestrate ovarian functional regulation.



Functional enrichment analysis of differentially expressed mRNA. (A) The X-axis denotes Gene Ontology (GO) terms, while the Y-axis represents the number of genes. Distinct color codes distinguish major GO categories, with darker colors corresponding to upregulated genes and lighter colors indicating downregulated genes; (B) each circle represents a KEGG pathway. The Y-axis shows pathway names, and the X-axis corresponds to the Rich Factor (defined as the ratio of the proportion of differentially expressed genes annotated to a specific pathway to the proportion of all genes annotated to that pathway).





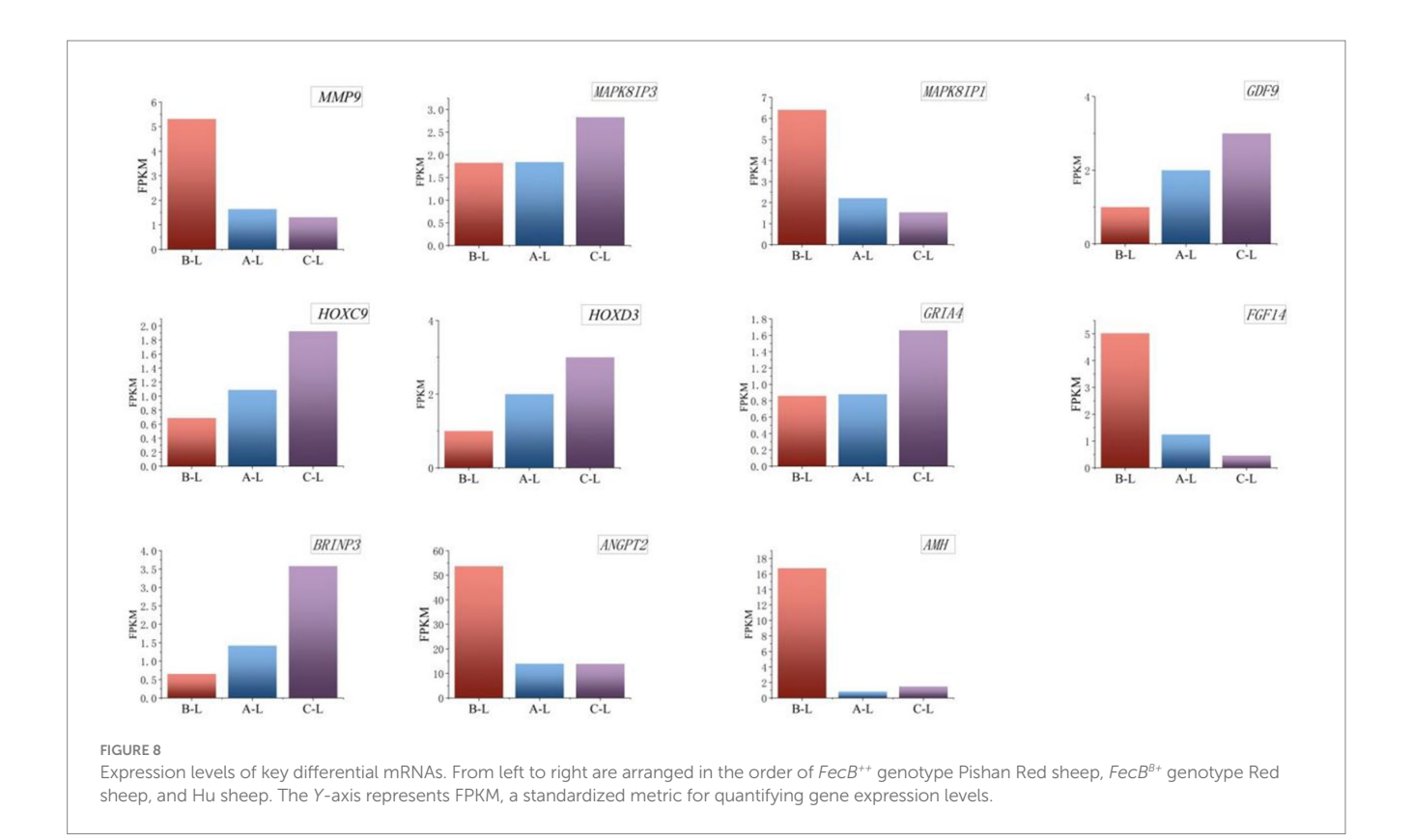
3.9 Screening of potential functional mRNAs and IncRNAs involved in the reproductive process

Functional enrichment analysis identified a cohort of significantly expressed mRNAs and lncRNAs in ovarian tissues during the estrous cycle, particularly enriched in key KEGG pathways including "Cytokine-cytokine receptor interaction," "Hippo signaling pathway," and "MAPK signaling pathway."

Transcriptomic profiling at the mRNA level identified critical genes – including *GDF9*, *GRIA4*, *HOXC9*, *HOXD3*, *MAPK8IP3*, *AMH*, *ANGPT2*, *FGF14*, *MAPK8IP1*, *MMP9*, and *BRINP3* demonstrating multifaceted roles in ovarian folliculogenesis, cell cycle modulation, and MAPK-mediated signal transduction cascades. Bar graph analysis of mRNA expression levels (Figure 8) revealed significant differences in gene expression across breeds, with these transcriptional disparities potentially linked to variations in their reproductive performance.

The AMH gene exhibited significantly higher expression levels in $FecB^{++}$ -genotype Pishan Red Sheep (Group B) compared to

FecB^{B+}-genotype (Group A) and Hu Sheep (Group C). This transcriptional pattern suggests that AMH may play a more prominent role in follicular quiescence regulation within mono-ovulatory breeds, while its activity in poly-ovulatory breeds is likely modulated through complementary regulatory mechanisms. The ANGPT2 gene displayed the highest expression levels in FecB++-genotype Pishan Red Sheep, compared to FecB^{B+}-genotype and Hu Sheep. This expression pattern may correlate with its dual roles in modulating ovarian angiogenesis and regulating follicular maturation during reproductive cycles. The FGF14 gene exhibited the highest expression levels in FecB++-genotype Pishan Red Sheep, whereas significantly lower expression was observed in FecB^{B+}-genotype and Hu Sheep. This differential expression pattern may be associated with FGF14's regulatory functions in cellular proliferation and differentiation. The HOXC9 and HOXD3 genes exhibited significantly lower expression levels in FecB⁺⁺-genotype Pishan Red Sheep compared to other genotypes, suggesting potential associations with their regulatory roles in embryonic morphogenesis and cellular differentiation processes. MAPK8IP1 and MMP9 exhibited the highest expression levels in



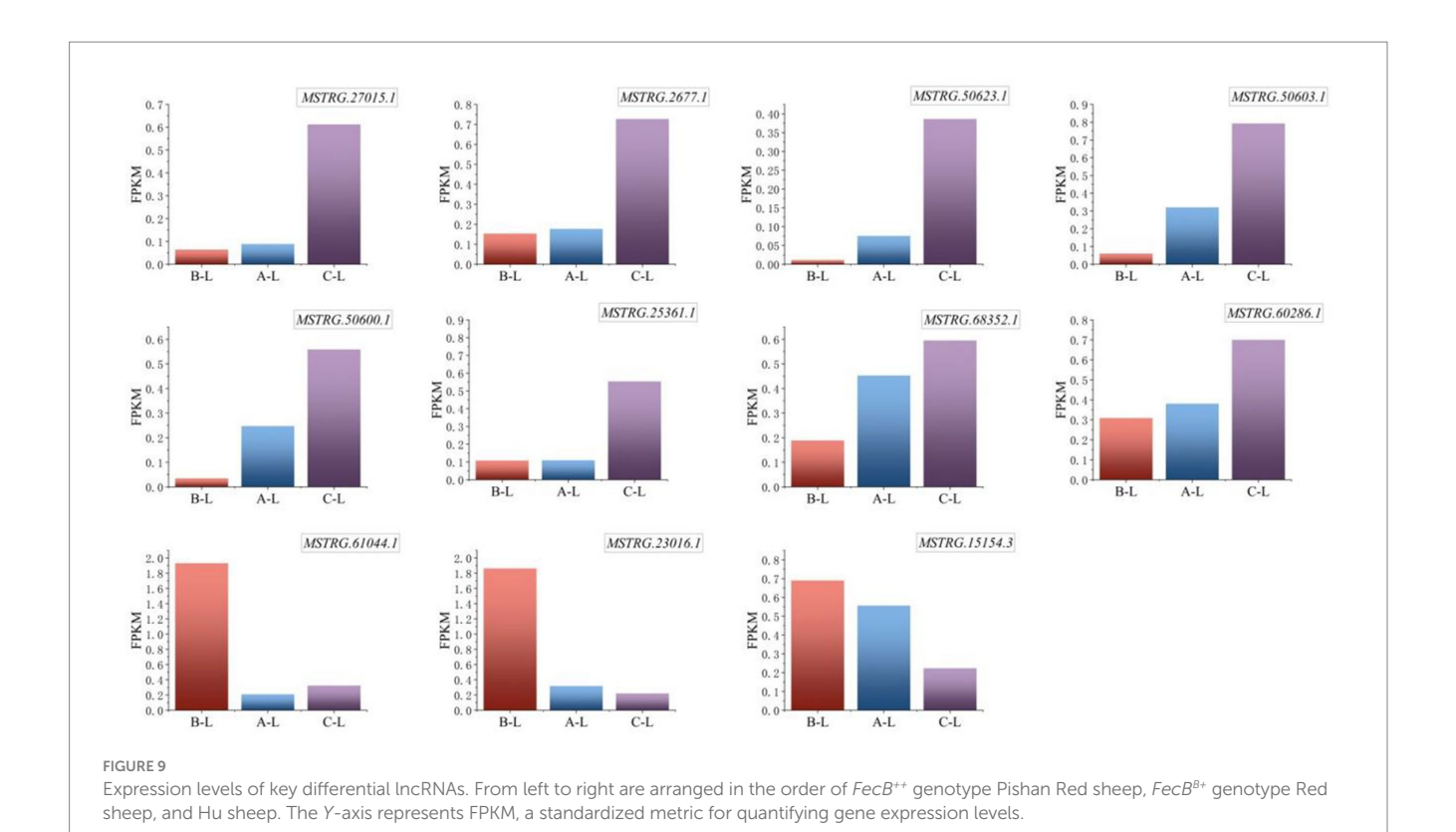
*FecB***-genotype Pishan Red Sheep, potentially linked to their functional roles in follicular maturation, ovulation dynamics, and extracellular matrix remodeling during ovarian tissue homeostasis.

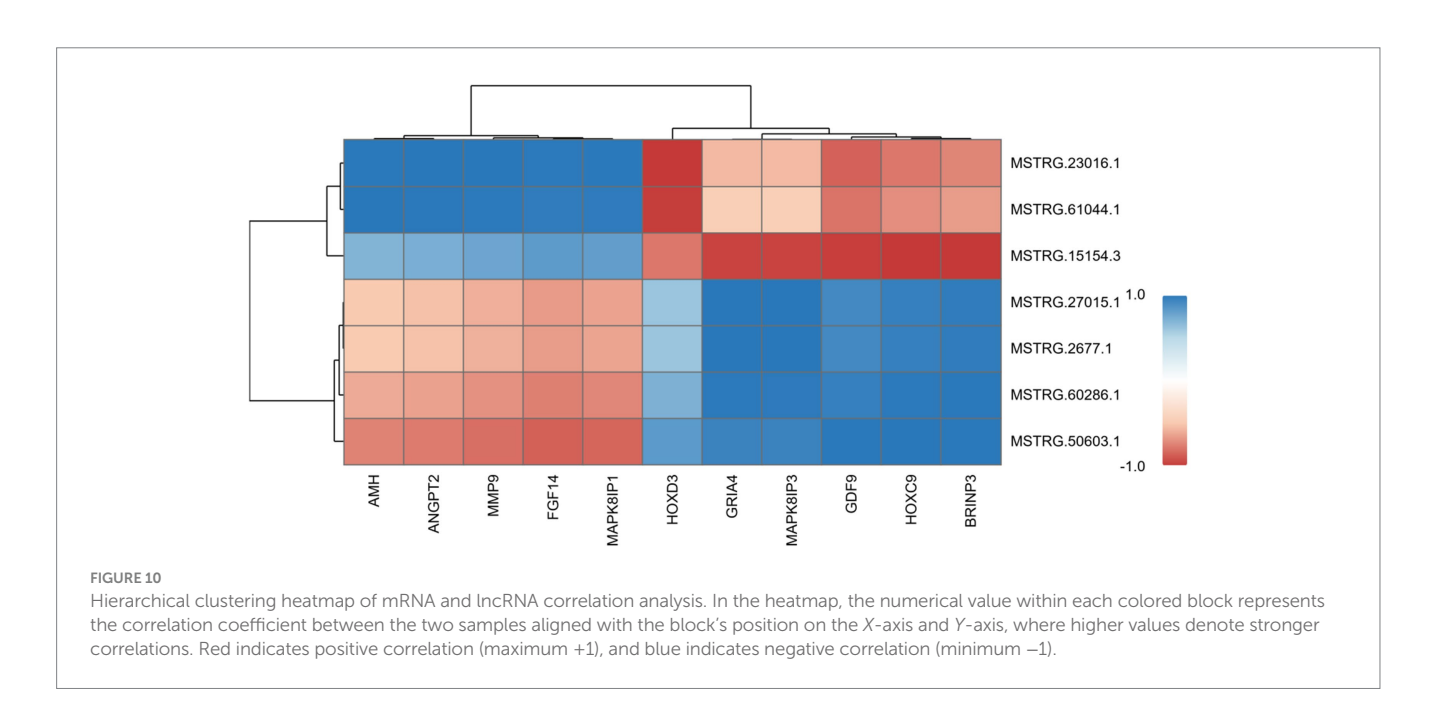
Critical lncRNAs identified through systematic analysis include *MSTRG.61044.1*, *MSTRG.2677.1*, *MSTRG.23016.1*, *MSTRG.27015.1*, *MSTRG.60286.1*, and *MSTRG.15154.3*, which exhibited conserved expression patterns across genotype groups. The results (Figure 9) demonstrated significant differential expression of these lncRNAs across ovine breeds, a transcriptional divergence potentially associated with their reproductive performance variations.

Specifically, the lncRNA MSTRG.61044.1, which is highly expressed in FecB++-genotype Pishan Red Sheep, demonstrates dual regulatory mechanisms: it exerts cis-regulatory control over the adjacent MAPK8IP1 gene, while trans-regulating reproductionassociated genes such as AMH and CCL25. These findings implicate MSTRG.61044.1 as a potential hub regulator orchestrating follicular selection and gonadotropin-responsive signaling cascades. Further investigation revealed that MSTRG.23016.1, also highly expressed in FecB++-genotype Pishan Red Sheep, exhibits functional modulation of MMP9 and ANGPT2 transcripts, suggesting its potential involvement in extracellular matrix remodeling and angiogenic niche regulation during ovarian tissue homeostasis. Simultaneously, MSTRG.15154.3 dynamically regulates granulosa cell proliferation and lineage commitment through cis-mediated transcriptional control of ERBB4, establishing a mechanistic link between lncRNA-driven chromatin interactions and follicular developmental competence. In contrast, Hu Sheep-specific highly expressed lncRNAs exhibited distinct functional orientations: MSTRG.2677.1 modulates ovarian stromal cell homeostasis through trans-regulation of HGF and BRINP3, potentially orchestrating extracellular matrix dynamics and stromal-epithelial crosstalk during follicular wave progression. *MSTRG.27015.1* and *MSTRG.60286.1* were found to target *MAPK8IP3* and *PPP3CB*, respectively. This mechanistic association suggests their potential roles in regulating cell cycle checkpoints and orchestrating oocyte maturation through calcium-dependent signaling cascades. Notably, MAPK signaling pathway-associated genes (*MAPK8IP1* and *MAPK8IP3*) exhibit breed-specific differential regulation by distinct lncRNAs, which may reflect evolutionary divergence in follicular development synchronization mechanisms across ovine breeds.

3.10 Key mRNA-lncRNA correlation analysis

Figure 10 demonstrates the correlation heatmap between key differentially expressed mRNAs and lncRNAs identified in this study. The heatmap revealed strong correlations between key differentially expressed mRNAs and lncRNAs, with these RNA molecules distinctly clustering into two groups based on their expression correlation patterns. Specifically, lncRNAs MSTRG.23016.1 and MSTRG.61044.1 demonstrated strong positive correlations with key reproductive regulators including AMH, ANGPT2, MMP9, FGF14, and MAPK8IP1, while exhibiting robust negative correlations with the HOXD3 gene. Furthermore, lncRNAs MSTRG.2677.1, MSTRG.27015.1, MSTRG.60286.1, and MSTRG.50603.1 exhibited strong positive correlations with GRIA4, MAPK8IP3, GDF9, HOXC9, and BRINP3 mRNAs. Notably, lncRNA MSTRG.50603.1 also exhibited strong negative correlations with MAPK8IP1, FGF14, and MMP9 mRNAs. Furthermore, MSTRG.15154.3 displayed strong positive correlations with FGF14 and MAPK8IP1, while showing negative correlations with

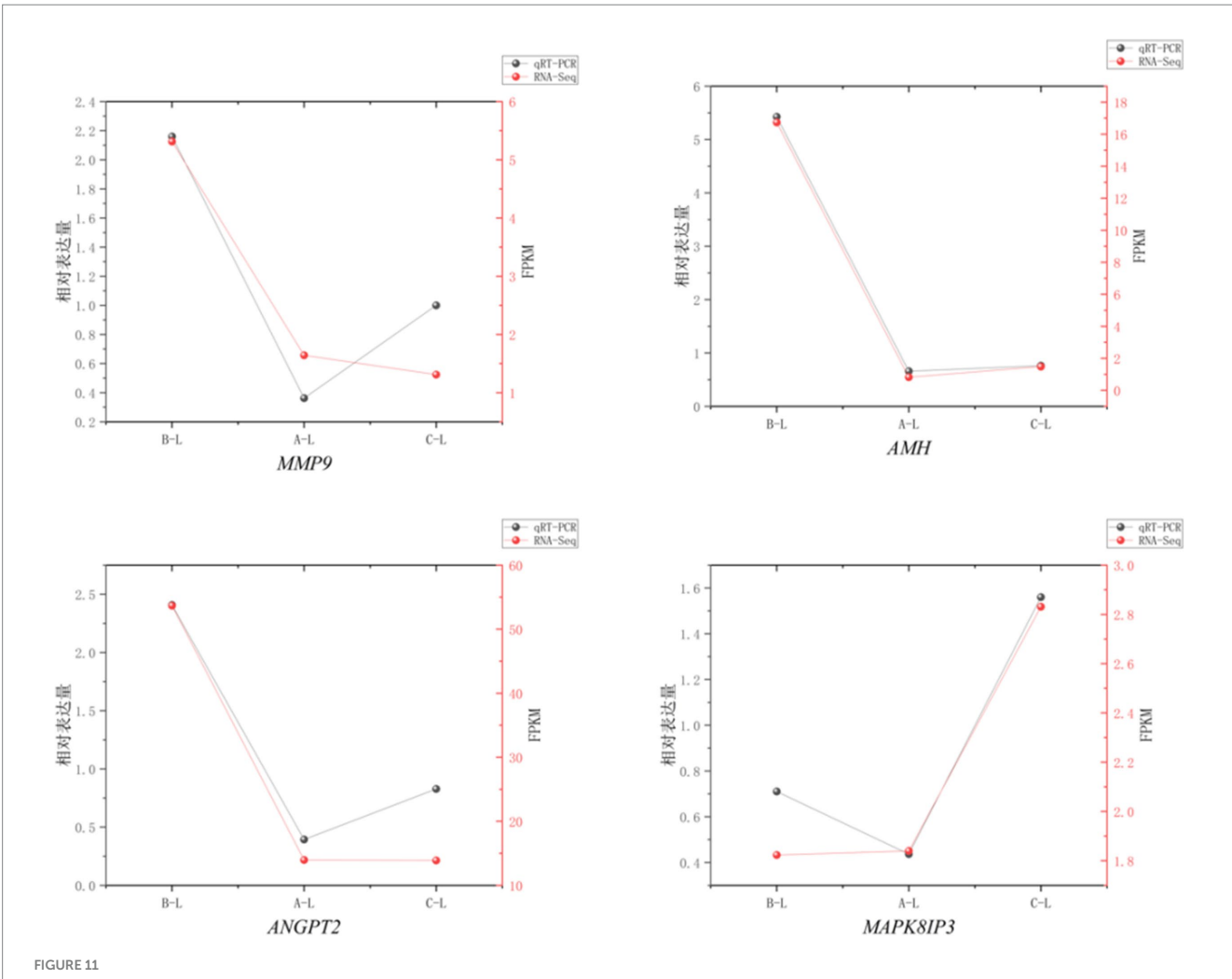




GRIA4, MAPK8IP3, GDF9, HOXC9, and BRINP3. Such correlation-based co-expression analysis has proven instrumental in pinpointing putative functional interactions within RNA regulatory networks, holding significant implications for deciphering transcriptional circuitry and elucidating molecular mechanisms governing ovarian folliculogenesis. These findings provide critical leads for subsequent functional validation studies, facilitating in-depth exploration of the intricate interplay between mRNAs and lncRNAs, as well as their roles in disease pathogenesis and progression.

3.11 Real-time quantitative PCR (RT-qPCR) validation

To assess the reliability of RNA sequencing, we randomly selected 4 mRNAs (*MMP9*, *AMH*, *ANGPT2*, *MAPK8IP3*) and 1 lncRNA (*MSTRG.60286.1*) for qRT-PCR validation. The results demonstrated consistent expression patterns across different reproductive stages between qRT-PCR and RNA-Seq data (Figures 11, 12), confirming the robustness of our transcriptomic analysis.

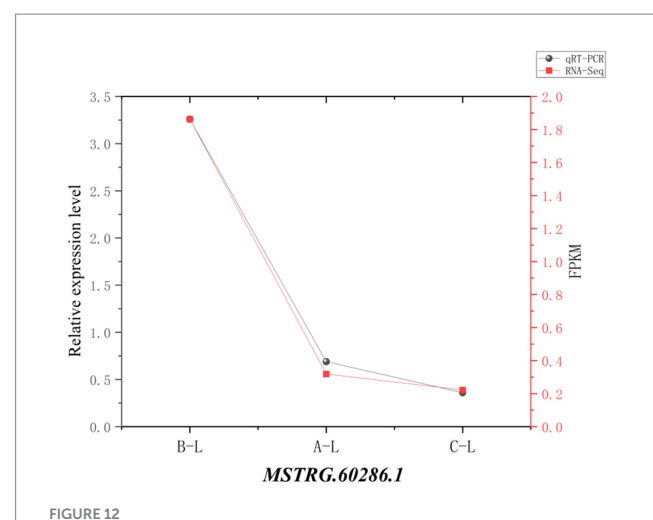


mRNA Real-time fluorescence quantitative PCR validation of RNA-Seq. Comparison of gene expression levels measured by qRT-PCR (black circles) and RNA-Seq (red squares). The *X*-axis represents different sample groups, arranged from left to right in the following order: *FecB*⁺⁺ genotype Pishan Red sheep, *FecB*⁸⁺ genotype Red sheep, and Hu sheep. The left *Y*-axis indicates the relative expression level (qRT-PCR), while the right y-axis shows the RNA-Seq-derived FPKM values.

4 Discussion

Research on ovine reproductive efficiency has revealed that elevated expression levels of genes such as GDF9 and BMP15 are intricately linked to follicular development, suggesting their potential as molecular targets for improving reproductive performance (21). In the present study, the highest expression level of the GDF9 gene was observed in Hu Sheep, followed by *FecB*^{B+} genotype Pishan Red Sheep, with the FecB++ genotype Pishan Red Sheep exhibiting the lowest expression. This finding suggests a potential positive correlation between GDF9 expression levels and ovine prolificacy, i.e., elevated expression may enhance fecundity traits. Xie et al. (22) discovered the pivotal role of the ELOVL7 gene in lipid metabolism in caudal fat. In this study, the high expression of GDF9 in ovarian tissue suggests its potential as a core regulatory node in reproduction control. Although ELOVL7 (lipid metabolism) and GDF9 (reproduction regulation) operate in distinct functional contexts, both influence cell fate by modulating key signaling pathways. This provides cross-phenotype research insights for elucidating the multi-tissue synergistic regulatory mechanisms underlying complex traits in sheep. Previous studies have demonstrated significant breed-specific variations in *GDF9* expression levels among ovine populations, with strong correlations observed between elevated expression and increased ovulation rates as well as improved litter size (21). Fengyan et al. (23) demonstrated that polymorphisms in the *GDF9* gene are significantly associated with litter size in Luzhong Meat Sheep, further reinforcing its critical role in modulating ovine prolificacy. Specifically, specific mutation loci in the *GDF9* gene are associated with increased litter sizes, suggesting that its expression level significantly influences ovine reproductive performance (24). This consensus aligns with the observed differential *GDF9* expression levels among ovine breeds in our study, empirically supporting its critical regulatory role in governing prolificacy traits.

MMP9 exhibits elevated expression levels in ovine ovarian tissues, with pronounced activity notably observed during follicular development (25). Elevated *MMP9* expression may facilitate follicular maturation and ovulation, thereby enhancing ovulation rates. Studies have revealed (26), that *MMP9* expression increases significantly during follicular maturation, with the



IncRNA real-time fluorescence quantitative PCR validation of RNA-Seq. Comparison of gene expression levels measured by qRT-PCR (black circles) and RNA-Seq (red squares). The X-axis represents different sample groups, arranged from left to right in the following order: $FecB^{++}$ genotype Pishan Red sheep, $FecB^{B+}$ genotype Red sheep, and Hu sheep. The left Y-axis indicates the relative expression level (qRT-PCR), while the right y-axis shows the RNA-Seq-derived FPKM values.

highest levels observed in the theca and granulosa cells of welldeveloped mature follicles. These findings collectively indicate that MMP9 likely plays a regulatory role in coordinating follicular development and ovulatory processes within ovine ovarian tissues, offering mechanistic insights into its contribution to reproductive efficiency. Studies have demonstrated that MMP9 deficient mice exhibit impaired embryonic development and dysregulated maternal-fetal interactions, characterized by intrauterine growth retardation and reduced litter size (27). This evidence strongly suggests that MMP9 exerts a critical regulatory influence on trophoblast cell differentiation and placental maturation, with functional perturbations in these processes directly contributing to compromised reproductive outcomes. Tight regulation of MMP9 expression is indispensable for maintaining physiological homeostasis, while dysregulated expression may be etiologically linked to reproductive pathologies such as impaired folliculogenesis and pregnancy disorders. MMP9 participates in uterine remodeling through extracellular matrix degradation, thereby influencing embryo implantation and pregnancy maintenance (28).

The elevated expression of *BRINP3* in ovine ovarian tissues and its marked differential expression in prolific sheep suggest its potential functional significance in mediating key reproductive processes. *BRINP3* may modulate the expression of gonadotropins, thereby regulating follicular development and ovulation. The elevated expression of *AMH* in ovine ovarian tissues and its pivotal role in follicular development suggest its potential critical function in regulating reproductive processes in sheep. Experimental results demonstrate that *AMH*-deficient mice exhibit significantly accelerated follicular depletion, providing direct evidence for the functional association between *AMH* and reproductive lifespan regulation (29). This study elucidates for the first time that *AMH* maintains the dynamic equilibrium of follicular development

through dual mechanisms: inhibiting primordial follicle recruitment and modulating follicle-stimulating hormone (FSH) receptor expression in granulosa cells. The establishment of an AMH-FSH-Inhibin B tripartite feedback regulatory system demonstrated that AMH suppresses FSH receptor expression in granulosa cells (with a 40% downregulation observed in vitro), thereby extending the survival duration of small antral follicles and augmenting ovulation potential (30). Qiang et al. (31) investigated the association between AMH genetic variants and reproductive performance in Lacaune sheep, identifying several single nucleotide polymorphisms (SNPs) significantly correlated with litter size. Hox genes, a highly conserved subgroup within the homeobox superfamily, play pivotal roles in developmental processes (32). Specifically, HOXC9 and HOXD3 are primarily responsible for orchestrating anterior-posterior axis formation and participate in the morphogenesis of specialized organ systems (33). Their expression typically exhibits marked temporal and spatial specificity, exerting profound regulatory effects on both the development and functional homeostasis of the reproductive system. Investigations into the expression patterns and functional roles of these genes provide critical insights into their potential regulatory mechanisms within ovine reproductive biology.

Studies have increasingly demonstrated that lncRNAs play indispensable roles in biological life cycles and reproductive processes (34, 35). Studies have revealed that lncRNAs are deeply involved in multiple reproductive processes, including ovarian development (36), oogenesis (37), and pregnancy maintenance (38), providing critical opportunities to investigate lncRNA-mediated regulation of ovine reproductive performance. In this study, comparative analysis of lncRNA and mRNA expression profiles in ovarian tissues during estrus between Pishan Red Sheep and Hu Sheep successfully identified key candidate mRNAs and their potentially regulatory lncRNAs. These findings further substantiate the pivotal role of lncRNAs in ovine reproduction.

lncRNAs regulate mRNA expression through both cis- and trans-acting mechanisms. Cis-acting lncRNAs modulate target gene expression through enhancer-like mechanisms, either activating or repressing transcription (39). Trans-acting lncRNAs regulate mRNA splicing, stability, and translation by interacting with proteins, DNA, and other RNAs (40). Xiaojing et al. (41) demonstrated that lipopolysaccharide (LPS) treatment induces significant alterations in the expression profiles of both lncRNAs and messenger RNAs (mRNAs) in bovine mammary epithelial cells. Zhang et al. (42) conducted RNA sequencing analysis of hypothalamic lncRNAs in Small Tail Han sheep carrying the FecB⁺⁺ genotype, identifying potential reproductive regulators such as MSTRG.26777 and MSTRG.105228. These findings provide novel insights into the hypothalamic regulation of ovine reproduction. The lncRNAs and mRNAs associated with ovine fecundity identified in our study corroborate the findings of Zhuangbiao Zhang et al., providing further evidence for the critical role of lncRNAs in sheep reproduction. Shabbir et al. (11) systematically characterized stage-specific lncRNA and mRNA expression profiles in Hu Sheep ovaries across follicular developmental stages, identifying differentially expressed miRNAs and lncRNAs that form potential regulatory networks. The identified genes are functionally implicated in ovarian follicular development and steroid hormone-mediated signaling pathways, among other

critical reproductive processes. These findings align with the roles of lncRNAs identified in our study—regulating follicular selection, hormonal response, ovarian tissue remodeling, and cellular proliferation/differentiation—collectively advancing the mechanistic understanding of ovine reproduction. However, functional validation of specific candidate genes remains warranted.

5 Conclusion

This study elucidates the molecular determinants of ovine reproductive efficiency through systematic analysis of differential expression profiles of lncRNAs and mRNAs in ovarian tissues during the estrous cycle between Pishan Red Sheep and Hu Sheep, unraveling key genetic regulators and their multifaceted mechanisms in follicular development and ovulation competency. A suite of key mRNAs, including GDF9, GRIA4, HOXC9, HOXD3, MAPK8IP3, AMH, ANGPT2, FGF14, MAPK8IP1, MMP9, and BRINP3, was successfully identified through systematic transcriptomic screening. Furthermore, we identified lncRNAs with regulatory interactions to these mRNAs, including MSTRG.61044.1, MSTRG.23016.1, MSTRG.15154.3, MSTRG.2677.1, MSTRG.27015.1, and MSTRG.60286.1. These lncRNAs exert critical regulatory roles in follicular selection, hormone responsiveness, ovarian tissue remodeling, and cellular proliferation/ differentiation through coordinated cis- and trans- regulatory mechanisms. The findings of this study establish a molecular framework for refining ovine reproductive management strategies and pinpoint critical gene regulatory hubs that may serve as pivotal modulators of reproductive efficiency.

Data availability statement

The RNA-Seq data of Pishan Red Sheep and Hu Sheep have been deposited in the Sequence Read Archive (SRA) database of the National Center for Biotechnology Information (NCBI) under BioProject accession number PRJNA1226111.

Ethics statement

The animal studies were approved by the experimental procedures and protocol of this study were approved by the Animal Ethics Review Committee of Xinjiang Agricultural University (2024027). The studies were conducted in accordance with the local legislation and institutional requirements. Written informed consent was obtained from the owners for the participation of their animals in this study.

Author contributions

AM: Writing – original draft, Conceptualization, Methodology, Formal analysis, Data curation. GG: Data curation, Validation, Writing – review & editing, Supervision, Project administration. YY: Writing – review & editing, Data curation, Methodology. AK: Data curation, Methodology, Software, Writing – review & editing. MZ: Writing – review & editing, Methodology, Formal analysis. QL: Supervision, Resources, Writing – review & editing. XD: Project

administration, Validation, Writing – review & editing. YS: Writing – review & editing, Funding acquisition, Supervision.

Funding

The author(s) declare that financial support was received for the research and/or publication of this article. This research was supported by the Natural Science Foundation of Xinjiang Uygur Autonomous Region (2024D01D08), the Major Science and Technology Special Project of Xinjiang Uygur Autonomous Region (2024A02004-1), and the Breeding and Extension Plan of High-Efficiency Mutton Sheep Varieties in the Agricultural Area of Xinjiang (XJARS-09-11).

Acknowledgments

We gratefully acknowledge the members of the laboratory for their suggestions and critical reading of the manuscript.

Conflict of interest

The authors declare that the research was conducted in the absence of any commercial or financial relationships that could be construed as a potential conflict of interest.

Generative AI statement

The authors declare that no Gen AI was used in the creation of this manuscript.

Any alternative text (alt text) provided alongside figures in this article has been generated by Frontiers with the support of artificial intelligence and reasonable efforts have been made to ensure accuracy, including review by the authors wherever possible. If you identify any issues, please contact us.

Publisher's note

All claims expressed in this article are solely those of the authors and do not necessarily represent those of their affiliated organizations, or those of the publisher, the editors and the reviewers. Any product that may be evaluated in this article, or claim that may be made by its manufacturer, is not guaranteed or endorsed by the publisher.

Supplementary material

The Supplementary material for this article can be found online at: https://www.frontiersin.org/articles/10.3389/fvets.2025.1614599/full#supplementary-material

SUPPLEMENTARY TABLE 1

Top five upregulated and downregulated mRNAs in estrus ovarian tissues.

SUPPLEMENTARY TABLE 2

Top five upregulated and downregulated IncRNAs in estrus ovarian tissues

References

- 1. ChengLong Z, Jihu Z, Mirenisa T, Qianqian C, Shudong L. Population structure, genetic diversity and prolificacy in Pishan Red Sheep under an extreme desert environment. *Front Genet*. (2023) 14:1092066. doi: 10.3389/fgene.2023.1092066
- 2. Tao Z, Dunying H, Qianjun Z, Siyuan Z, Linjie W, Li L, et al. Comparative whole-genome resequencing to uncover selection signatures linked to litter size in Hu sheep and five other breeds. *BMC Genomics*. (2024) 25:480. doi: 10.1186/s12864-024-10396-x
- 3. Wang X, Li W, Huang Q, Sun H, Zhu L, Gu R, et al. Genomic signal selection analysis reveals genes related to the lambing trait of Hotan sheep. *Anim Biosci.* (2024) 38:1384–97. doi: 10.5713/ab.24.0336
- 4. Notter DR. Genetic aspects of reproduction in sheep. *Reprod Domest Anim.* (2008) 43:122–8. doi: 10.1111/j.1439-0531.2008.01151.x
- 5. Ekiz B, Ozcan M, Yilmaz A, Ceyhan A. Estimates of phenotypic and genetic parameters for ewe productivity traits of Turkish merino (Karacabey merino) sheep. *Turk Vet Hayvan Derg.* (2005) 29:557–64.
- 6. Tao M, Li Z, Liu M, Ma H, Liu W. Association analysis of polymorphisms in SLK, ARHGEF9, WWC2, GAB3, and FSHR genes with reproductive traits in different sheep breeds. *Front Genet.* (2024) 15:1371872. doi: 10.3389/fgene.2024.1371872
- 7. Haiguang M, Lu C, Rupo B, Shiqiao W, Mengting W, Ningying X, et al. Mechanisms of oogenesis-related long non-coding RNAs in porcine ovaries treated with recombinant pig follicle-stimulating hormone. *Front Vet Sci.* (2022) 8:838703. doi: 10.3389/fvets.2021.838703
- 8. Braga EA, Fridman MV, Burdennyy AM, Loginov VI, Dmitriev AA, Pronina IV, et al. Various LncRNA mechanisms in gene regulation involving miRNAs or RNA-binding proteins in non-small-cell lung cancer: main signaling pathways and networks. *Int J Mol Sci.* (2023) 24:13617. doi: 10.3390/ijms241713617
- 9. Yashpal R, Ma P, Jasbir D, Melcy P, Levin K, Sonika T. Linc2function: a comprehensive pipeline and webserver for long non-coding RNA (lncRNA) identification and functional predictions using deep learning approaches. *Epigenomes*. (2023) 7:22. doi: 10.3390/epigenomes7030022
- 10. Herman AB, Tsitsipatis D, Gorospe M. Integrated lncRNA function upon genomic and epigenomic regulation. *Mol Cell.* (2022) 82:2252–66. doi: 10.1016/j.molcel.2022.05.027
- 11. Shabbir S, Boruah P, Xie L, Kulyar MFEA, Nawaz M, Yousuf S, et al. Genome-wide transcriptome profiling uncovers differential miRNAs and lncRNAs in ovaries of hu sheep at different developmental stages. *Sci Rep.* (2021) 11:5865. doi: 10.1038/s41598-021-85245-v
- $12.\,Lamond$ DR, Bindon BM. Effect of nutrient intake on ovulation in mice and sheep. Biol Reprod. (1969) 1:264. doi: 10.1095/biolreprod. 3.264
- 13. Scaramuzzi RJ, Baird DT, Campbell BK, Driancourt MA, Dupont J, Fortune JE, et al. Regulation of Folliculogenesis and the determination of ovulation rate in ruminants. *Reprod Fertil Dev.* (2011) 23:444. doi: 10.1071/RD09161
- 14. Wang Y, Chao T, Li Q, He P, Zhang L, Wang J. Metabolomic and transcriptomic analyses reveal the potential mechanisms of dynamic ovarian development in goats during sexual maturation. *Int J Mol Sci.* (2024) 25:9898. doi: 10.3390/ijms25189898
- 15. Zheng M, Andersen CY, Rasmussen FR, Cadenas J, Christensen ST, Mamsen LS. Expression of genes and enzymes involved in ovarian steroidogenesis in relation to human follicular development. *Front Endocrinol.* (2023) 14:1268248. doi: 10.3389/fendo.2023.1268248
- 16. Zijing Z, Qiaoting S, Xiaoting Z, Lei J, Limin L, Shijie L, et al. Identification and functional analysis of transcriptome profiles, long non-coding RNAs, single-nucleotide polymorphisms, and alternative splicing from the oocyte to the preimplantation stage of sheep by single-cell RNA sequencing. *Genes.* (2023) 14:1145. doi: 10.3390/genes14061145
- 17. Cao C, Zhou Q, Kang Y, Akhatayeva Z, Liu P, Bai Y, et al. A repertoire of single nucleotide polymorphisms (SNPs) of major fecundity BMPR1b gene among 75 sheep breeds worldwide. *Theriogenology*. (2024) 219:59–64. doi: 10.1016/j.theriogenology.2024.02.019
- 18. Si C, Xiaofei G, Xiaoyun H, Ran D, Xiaosheng Z, Jinlong Z, et al. Transcriptome analysis reveals differentially expressed genes and long non-coding RNAs associated with fecundity in sheep hypothalamus with different FecB genotypes. *Front Cell Dev Biol.* (2021) 9:633747. doi: 10.3389/fcell.2021.633747
- 19. Ma K, Song J, Li D, Li T, Ma Y. Genetic diversity and selection signal analysis of Hu sheep based on SNP50K Beadchip. *Animals*. (2024) 14:2784. doi: 10.3390/ani14192784
- 20. Zhen W, Hua Y, Yu C, Jianyu M, Peiyong C, Zhibo W, et al. Comparative transcriptomic analysis of Hu sheep pituitary gland prolificacy at the follicular and luteal phases. *Genes*. (2022) 13:440. doi: 10.3390/genes13030440
- 21. Chen Y, Shan X, Jiang H, Sun L, Guo Z. Regulation of litter size in sheep (*Ovis aries*) by the GDF9 and BMP15 genes. *Ann Agric Sci.* (2023) 68:148–58. doi: 10.1016/j.aoas.2023.12.004

- 22. Xie Y, Li X, Liang H, Chu M, Cao G, Jiang Y. Integrated multiomic profiling of tail adipose tissue highlights novel genes, lipids, and metabolites involved in tail fat deposition in sheep. *BMC Genomics*. (2025) 26:212. doi: 10.1186/s12864-025-11380-9
- 23. Fengyan W, Mingxing C, Linxiang P, Xiangyu W, Xiaoyun H, Rensen Z, et al. Polymorphism detection of GDF9 gene and its association with litter size in Luzhong mutton sheep (*Ovis aries*). *Animals*. (2021) 11:571. doi: 10.3390/ani11020571
- 24. Tong B, Wang J, Cheng Z, Liu J, Wu Y, Li Y, et al. Novel variants in GDF9 gene affect promoter activity and litter size in Mongolia sheep. Genes. (2020) 11:375. doi: 10.3390/genes11040375
- Puttabyatappa M, Irwin A, Martin JD, Mesquitta M, Veiga-Lopez A, Padmanabhan V. Developmental programming: gestational exposure to excess testosterone alters expression of ovarian matrix metalloproteases and their target proteins. *Reprod Sci.* (2018) 25:882–92. doi: 10.1177/1933719117697127
- 26. Zhu G, Kang L, Wei Q, Cui X, Wang S, Chen Y, et al. Expression and regulation of MMP1, MMP3, and MMP9 in the chicken ovary in response to gonadotropins, sex hormones, and TGFB11. *Biol Reprod.* (2014) 90. doi: 10.1095/biolreprod.113.114249
- 27. Plaks V, Rinkenberger J, Dai J, Flannery M, Sund M, Kanasaki K, et al. Matrix Metalloproteinase-9 deficiency phenocopies features of preeclampsia and intrauterine growth restriction. *Proc Natl Acad Sci.* (2013) 110:11109–14. doi: 10.1073/pnas.1309561110
- 28. Nothnick WB. Regulation of uterine matrix Metalloproteinase-9 and the role of microRNAs. Semin Reprod Med. (2008) 26:494-9. doi: 10.1055/s-0028-1096129
- 29. Durlinger AL, Kramer P, Karels B, de Jong FH, Uilenbroek JT, Grootegoed JA, et al. Control of primordial follicle recruitment by anti-Müllerian hormone in the mouse ovary. *Endocrinology*. (1999) 140:5789–96. doi: 10.1210/endo.140.12.7204
- 30. Turgut AO, Koca D. Anti-Müllerian hormone as a promising novel biomarker for litter size in Romanov sheep. *Reprod Domest Anim.* (2024) 59:e14692. doi: 10.1111/rda.14692
- 31. Qiang D, Chuang Q, YuanYuan Z, XueJun S, XiaoLiang L. A novel AMH variant at the prehelix loop impairs the binding to AMHR2 and causes persistent Müllerian duct syndrome. *Asian J Androl.* (2023) 26:222–4. doi: 10.4103/aja202362
- 32. Nilay S, Saraswati S. The hox genes and their roles in oncogenesis. *Nat Rev Cancer*. (2010) 10:361–71. doi: 10.1038/nrc2826
- 33. Ne L, Km A. There and back again: hox clusters use both DNA strands. J Dev Biol. (2021) 9:28. doi: 10.3390/jdb9030028
- 34. Jiangzhou Z, Shuheng B, Yanli Y, Haojing K, Guangzu L, Zhaode F, et al. Construction of lncRNA-m6A gene-mRNA regulatory network to identify m6A-related lncRNAs associated with the progression of lung adenocarcinoma. *BMC Pulm Med*. (2023) 23:284. doi: 10.1186/s12890-023-02545-x
- 35. Xu W, Lin J, Faqiong X, Sumei C, Yuan C, Yingyan Z, et al. Long noncoding RNAs profiling in ovary during laying and nesting in Muscovy ducks (*Cairina moschata*). *Anim Reprod Sci.* (2021) 230:106762. doi: 10.1016/j.anireprosci.2021.106762
- 36. Dongyong Y, Yanqing W, Yajing Z, Fangfang D, Shiyi L, Mengqin Y, et al. Silencing of IncRNA UCA1 inhibited the pathological progression in Pcos mice through the regulation of PI3K/AKT signaling pathway. *J Ovarian Res.* (2021) 14:48. doi: 10.1186/s13048-021-00792-2
- 37. Yerushalmi GM, Salmon-Divon M, Yung Y, Maman E, Kedem A, Ophir L, et al. Characterization of the human cumulus cell transcriptome during final follicular maturation and ovulation. $Mol\ Hum\ Reprod.\ (2014)\ 20:719–35.\ doi: 10.1093/molehr/gau031$
- 38. Su T, Yu H, Luo G, Wang M, Zhou C, Zhang L, et al. The interaction of lncRNA XLOC-2222497, AKR1C1, and progesterone in porcine endometrium and pregnancy. *Int J Mol Sci.* (2020) 21:3232. doi: 10.3390/ijms21093232
- 39. Clark MB, Amaral PP, Schlesinger FJ, Dinger ME, Taft RJ, Rinn JL, et al. The reality of pervasive transcription. *PLoS Biol.* (2011) 9:discussion e1102. doi: 10.1371/journal.pbio.1000625
- 40. Elcheva IA, Spiegelman VS. The role of cis- and trans-acting RNA regulatory elements in Leukemia. Cancers~(Basel).~(2020)~12:3854.~doi:~10.3390/cancers12123854
- 41. Xiaojing X, Jie H, Pengfei R, Mingcheng L, Lei W, Xiaobing W, et al. Coexpression analysis of IncRNAs and mRNAs identifies potential regulatory long noncoding RNAs involved in the inflammatory effects of lipopolysaccharide on bovine mammary epithelial cells. *BMC Vet Res.* (2023) 19:209. doi: 10.1186/s12917-023-03780-4
- 42. Zhang Z, Tang J, Di R, Liu Q, Wang X, Gan S, et al. Comparative transcriptomics reveal key sheep (*Ovis Aries*) hypothalamus Lncrnas that affect reproduction. *Animals*. (2019) 9:152. doi: 10.3390/ani9040152